Structural Engineering and Mechanics, *Vol. 59, No. 1 (2016) 187-207*
DOI: http://dx.doi.org/10.12989/sem.2016.59.1.187

Operational modal analysis of structures by stochastic subspace identification with a delay index

Dan Li[1,2], Wei-Xin Ren[*1], Yi-Ding Hu[3] and Dong Yang[1]

[1]*School of Civil Engineering, Hefei University of Technology, Hefei, 230009, China*
[2]*Department of Civil and Environmental Engineering, National University of Singapore, 117576, Singapore*
[3]*School of Information Engineering, Wuyi University, Jiangmen, 529020, China*

(Received May 3, 2015, Revised April 20, 2016, Accepted April 29, 2016)

Abstract. Practical ambient excitations of engineering structures usually do not comply with the stationary-white-noise assumption in traditional operational modal analysis methods due to heavy traffic, wind guests, and other disturbances. In order to eliminate spurious modes induced by non-white noise inputs, the improved stochastic subspace identification based on a delay index is proposed in this paper for a representative kind of stationary non-white noise ambient excitations, which have nonzero autocorrelation values near the vertical axis. It relaxes the stationary-white-noise assumption of inputs by avoiding corresponding unqualified elements in the Hankel matrix. Details of the improved stochastic subspace identification algorithms and determination of the delay index are discussed. Numerical simulations on a four-story frame and laboratory vibration experiments on a simply supported beam have demonstrated the accuracy and reliability of the proposed method in eliminating spurious modes under non-white noise ambient excitations.

Keywords: operational modal analysis; non-white noise ambient excitations; stochastic subspace identification; delay index

1. Introduction

As the basis of dynamic analysis, finite element model updating and damage detection, modal parameter identification plays an important role in structural health monitoring (Hassiotis 1999, Van der Auweraer and Hermans 1999). For civil engineering structures, operational modal analysis has become more and more popular because of its applicable and economic benefits (De Roeck *et al*. 2000, Ren and Zong 2004). It dispenses with artificial excitation, and relies on ambient vibration measurements, which represent the actual operating conditions of structures. Consequently, operational modal parameter identification methods have to process very small magnitudes of vibration responses affected by unknown ambient excitations with stochastic noises. After several decades of development, researches in operational modal analysis are now focused on enhancing the accuracy of estimated results in practical application where noises inevitably exist (Dorvash and Pakzad 2012, Reynders 2012).

*Corresponding author, Professor, E-mail: renwx@hfut.edu.cn

http://www.techno-press.org/?journal=sem&subpage=8 ISSN: 1225-4568 (Print), 1598-6217 (Online)

Traditional operational modal analysis methods, such as frequency domain decomposition (FDD), peak picking (PP), auto regressive moving average (ARMA) model, natural excitation technique (NExT), and stochastic subspace identification (SSI), all assume that the unmeasured ambient excitations are stationary white stochastic processes (Yi and Yun 2004). For instance, in stochastic subspace identification method, the stationary-white-noise assumption of inputs helps to establish direct relationships between dynamic response and structural characteristics, based on which system parameters could be identified by singular value decomposition (SVD) and other numerical techniques (Peeters and De Roeck 2001, Ren *et al*. 2004). However, actual ambient excitations of engineering structures under operational conditions usually behave with obvious non-whiteness and even non-stationarity. They usually contain dominant frequencies due to heavy traffic, wind gusts, and other disturbances. Some incidental but prominent disturbances may even take place, like typhoons and earthquakes. As a result, those non-white components would bring spurious modes and calculation errors into the results of traditional operational modal parameter identification methods (Peeters 2000, Mevel *et al*. 2002, Li *et al*. 2011). Elimination of spurious modes is not easy due to the complexity and insufficient knowledge of operational excitations, especially when both of the structural and spurious modes are mixed in close frequency domain.

Lisowski (2001) summarized the characteristics of structural vibration modes compared to harmonic modes in practice, i.e., fast decay, higher mode shape complexity, constant time-frequency representation, and mutual linear independence, which are used as criteria to identify structural modes. As most of the researchers, Reynders *et al*. (2008) assumed that those spurious modes due to constant harmonic components in the inputs normally have zero damping ratios and so can be discriminated from structural modes in the final identification results. Brincker *et al*. (2001) pointed out that, in the frequency domain decomposition method, a harmonic frequency would produce peaks in nearly all singular values of the power spectral density (PSD) matrix, while eigenfrequencies only produce peaks at the first singular value. Jacobsen (2005) stated that the probability density function (PDF) of a structural mode is normally distributed, while that of a pure harmonic component will have two distinct peaks approaching infinity at ±A, where A is the amplitude of the harmonic component. Besides, Mohanty and Rixen (2004a, 2004b, 2006) have modified least squares complex exponential (LSCE), Ibrahim time domain (ITD) and eigensystem realization algorithm (ERA), which are carried out along with the NExT for operational modal analysis, to explicitly take into account the effect of purely harmonic vibrations. Unfortunately, they all depend on a threshold that the harmonic frequencies must be known in advance, which is not applicable for civil engineering structures in intricate ambient.

However, unlike machines with rotating or reciprocating parts, non-white components in ambient excitations of civil engineering structures may not be standard harmonics that are stably lasting without damping. It has been acknowledged by experiments that the dampings of harmonic frequencies identified in practice are not too small to be ignored, and direct filtering of harmonic components would pollute the measured responses, especially when they are close to structural eigenfrequencies. By combining transmissibility measurements under different loading conditions, a novel approach has been proposed by Devriendt *et al.* (2007, 2009), which does not rely on any assumption about the ambient excitations. Recently, other researchers are trying to improve it in order to avoid the need of multiple loading conditions that are inconvenient and even impossible for practical applications (Yan and Ren 2013, Araújo and Laier 2014).

For stochastic subspace identification, one of the most advanced operational modal analysis methods, some relevant efforts have been made for the sake of accurate identification results in case of various noises. The most significant improvement is the introduction of stabilization

diagram (Van Overschee and De Moor 1996, Peeters and De Roeck 2001), in which spurious frequencies from numerical and ambient noises would not stabilize with the increase of model order according to the preset limits of modal parameters. Goethals *et al*. (2004) investigated an automatic interpretation algorithm for the stabilization diagrams in stochastic subspace identification that separates the physical and spurious modes through a simple clustering technique and a self-learning classification algorithm. Yu and Ren (2005) combined the empirical mode decomposition (EMD) technique with stochastic subspace identification to bypass spurious frequencies due to unwanted noises. Goursat and Mevel (2008) pointed out that the damping ratio and mode shape sometimes are of no help to distinguish the true modes of structural system from spurious ones, and then proposed to check the stability of identified modes for different windows on measurement data. Saeed *et al*. (2008) suggested an alternative stabilization histogram to reject spurious modes by combining identified results from the measured output signals of different sampling rates. Nonetheless, these techniques above based on the stabilization diagram in stochastic subspace identification are mainly effective for spurious modes generated by measurement noises and numerical calculation.

Obviously, the operational modal parameter identification of engineering structures under non-white noise ambient excitations is still a challenging task. More complicated types of non-white noises should be considered that do not stably last without damping as standard harmonics, and that could not be recognized by existing techniques like stabilization diagram theory and zero-damping criterion. This paper focuses on the stationary non-white noise excitations, specifically a representative kind of practical non-white noises with nonzero autocorrelation values near the vertical axis, which involves many forms in time domain, like colored noises, swept harmonics, impacts, and etc (Cooper *et al*. 1995). By introducing a delay index, the improved stochastic subspace identification is developed for engineering structures under such non-white noise ambient excitations. Details of the improved identification algorithms and determination of the delay index are illustrated. Numerical simulations on a four-story frame and laboratory vibration experiments on a simply supported beam have demonstrated that the proposed improved stochastic subspace identification based on a delay index is able to eliminate spurious modes induced by non-white noise excitations. It relaxes the traditional stationary-white-noise assumption of ambient excitations in operational modal analysis, and improves the precision of identification results.

2. Traditional stochastic subspace identification procedures

The widely-used stochastic subspace identification has two branches: covariance-driven method and data-driven method. Both of these two algorithms rely on the stochastic state space model of vibrating system, while the differences between them are detailed techniques adopted for reducing measurement data and solving system of equations. This section briefly describes the two identification procedures, and more detailed information could be found in the references (Van Overschee and De Moor 1996, Peeters 2000, Ren *et al*. 2004).

2.1 Stochastic state space model of a vibrating system

The dynamic model of a structure, i.e., a vibrating system, can be converted to the discrete-time stochastic state space model, by applying model reduction, sampling and modelling the noise

$$\begin{cases} x_{k+1} = Ax_k + w_k \\ y_k = Cx_k + v_k \end{cases} \tag{1}$$

where k is the discrete time instant; x_k is the discrete state vector; y_k is the sampled output vector (measurements). A is the discrete state matrix that fully characterizes the dynamics of the system by its eigenvalues. C is the discrete output matrix that specifies how the internal states are transformed to the outside world. w_k is the process noise typically due to processing disturbances and modeling inaccuracies, but here also due to the unknown ambient excitation of the structure. v_k is the measurement noise typically due to sensor inaccuracy, but here also due to the unknown ambient excitation of the structure (Peeters and De Roeck 2001).

The two noise terms, w_k and v_k, implicitly involving the ambient inputs, are both unmeasurable signals assumed to be stationary white noises with zero means and covariance matrices

$$\mathrm{E}\left[\begin{pmatrix} w_p \\ v_p \end{pmatrix}\begin{pmatrix} w_q^T & v_q^T \end{pmatrix}\right] = \begin{pmatrix} Q & S \\ S^T & R \end{pmatrix}\delta_{pq} \tag{2}$$

where δ_{pq} is the Kronecker delta. This stationary-white-noise assumption cannot be omitted for the sake of accurate system identification results in both of the traditional covariance-driven and data-driven stochastic subspace identification methods. If the ambient excitations contain some dominant frequency components, these frequency components will appear as spurious poles of the state matrix A and cannot be separated from intrinsic modes of the system (Van Overschee and De Moor 1996, Peeters 2000). Based on the stationary-white-noise assumption of ambient excitations, a recursive relationship between output covariances (i.e. autocorrelation function for stochastic processes with zero means) $R_i = \mathrm{E}[y_{k+i}y_k^T]$ and system state matrix A is obtained

$$\begin{cases} R_i = CA^{i-1}G \\ R_{-i} = G^T\left(A^{i-1}\right)^T C^T \end{cases} \qquad (i = 1, 2, 3\cdots) \tag{3}$$

Here, $G = \mathrm{E}[x_{k+1}y_k^T]$ is the covariance matrix between next state and output.

2.2 Covariance-driven stochastic subspace identification (SSI-COV)

In short, the covariance-driven stochastic subspace identification can be implemented in the following six steps (Peeters 2000).

(1) Form the Hankel matrix $(Y_{0|i-1}/Y_{i|2i-1}) \in \mathbf{R}^{2li\times j}$ using output measurements according to predefined index i and j, where l is the number of output channels.

$$\begin{pmatrix} Y_{0|i-1} \\ \hline Y_{i|2i-1} \end{pmatrix} = \begin{pmatrix} Y_p \\ \hline Y_f \end{pmatrix} = \frac{1}{\sqrt{j}}\left(\begin{array}{ccccc} y_0 & y_1 & y_2 & \cdots & y_{j-1} \\ y_1 & y_2 & y_3 & \cdots & y_j \\ \cdots & \cdots & \cdots & \cdots & \cdots \\ y_{i-1} & y_i & y_{i+1} & \cdots & y_{i+j-2} \\ \hline y_i & y_{i+1} & y_{i+2} & \cdots & y_{i+j-1} \\ y_{i+1} & y_{i+2} & y_{i+3} & \cdots & y_{i+j} \\ \cdots & \cdots & \cdots & \cdots & \cdots \\ y_{2i-1} & y_{2i} & y_{2i+1} & \cdots & y_{2i+j-2} \end{array}\right) \tag{4}$$

It should be noted that the matrix has been divided into past part Y_p and future part Y_f.

(2) Calculate the Toeplitz matrix $T_{1|i} \in \mathbf{R}^{li \times li}$.

$$T_{1|i} = Y_f Y_p^T = \begin{pmatrix} R_i & R_{i-1} & ... & R_1 \\ R_{i+1} & R_i & ... & R_2 \\ ... & ... & ... & ... \\ R_{2i-1} & R_{2i-2} & ... & R_i \end{pmatrix} \tag{5}$$

(3) Singular value decomposition of the Toeplitz matrix.

$$T_{1|i} = USV^T = \begin{pmatrix} U_1 & U_2 \end{pmatrix} \begin{pmatrix} S_1 & 0 \\ 0 & S_2 = 0 \end{pmatrix} \begin{pmatrix} V_1 \\ V_2 \end{pmatrix} = U_1 S_1 V_1^T \tag{6}$$

The rank of Toeplitz matrix indicates the order of structural system, n.

(4) Deduce the extended observability matrix O_i and reversed extended stochastic controllability matrix Γ_i.

$$T_{1|i} = \begin{pmatrix} C \\ CA \\ ... \\ CA^{i-1} \end{pmatrix} \begin{pmatrix} A^{i-1}G & ... & AG & G \end{pmatrix} = O_i \Gamma_i \tag{7}$$

where

$$O_i = U_1 S_1^{1/2}, \quad \Gamma_i = S_1^{1/2} V_1^T \tag{8}$$

(5) Estimate the system matrices A and C.

Another Toeplitz matrix $T_{2|i+1}$ is calculated from a new Hankel matrix ($Y_{0|i\text{-}1}/Y_{i+1|2i}$), and compared with $T_{1|i}$ in order to obtain the system matrices.

$$T_{2|i+1} = O_i A \Gamma_i \tag{9}$$

$$A = S_1^{-1/2} U_1^T T_{2|i+1} V_1 S_1^{-1/2}, \quad C = O_i \left(1:l,:\right) \tag{10}$$

(6) Identify the modal parameters.

The eigenvalues of discrete and continuous state matrices, A and A_c, are respectively μ_i and λ_i, which correspond to the same eigenvector matrix Ψ.

$$A = \Psi \Lambda \Psi^{-1}, \ \Lambda = diag[\mu_i] \in \mathbf{C}^{n \times n}, \ \lambda_i = \frac{\ln \mu_i}{\Delta t} \tag{11}$$

Finally, the frequencies, damping ratios and mode shapes of a vibrating system are identified.

$$\omega_i = \sqrt{\left(\lambda_i^R\right)^2 + \left(\lambda_i^I\right)^2}, \quad \xi_i = -\frac{\lambda_i^R}{\sqrt{\left(\lambda_i^R\right)^2 + \left(\lambda_i^I\right)^2}}, \quad V = C\Psi \tag{12}$$

2.3 Data-driven stochastic subspace identification (SSI-DATA)

By applying the Kalman filter to the stochastic state space model, a forward innovation model is established, and then an optimal prediction of the state vector x_k, denoted as $\hat{x}_k$ (k=1,2...), is produced by utilizing observations of the outputs up to time $k-1$ and the available system matrices together with the known noise covariances. Eq. (13) below defines the Kalman filter state sequence $\hat{X}_i \in \mathbf{R}^{n\times j}$, and its relationship with the state matrix and output of system

$$\hat{X}_i = \begin{pmatrix} \hat{x}_i & \hat{x}_{i+1} & \cdots & \hat{x}_{i+j-1} \end{pmatrix} = \begin{pmatrix} A^{i-1}G & \ldots & AG & G \end{pmatrix} \begin{pmatrix} R_0 & R_{-1} & \ldots & R_{1-i} \\ R_1 & R_0 & \ldots & R_{2-i} \\ \ldots & \ldots & \ldots & \ldots \\ R_{i-1} & R_{i-2} & \ldots & R_0 \end{pmatrix} Y_p \tag{13}$$

where Y_p is the past part of Hankel matrix. In the light of these ideas, the data-driven stochastic subspace identification can be represented by the following six steps (Peeters 2000).

(1) Form the Hankel matrix $(Y_{0|i-1} / Y_{i|2i-1}) \in \mathbf{R}^{2li\times j}$ same as Eq. (4).

(2) Project the row space of future outputs into that of past outputs through QR decomposition.

$$\mathrm{P}_i = Y_f / Y_p = Y_f Y_p^T \left(Y_p Y_p^T\right)^{\dagger} Y_p = \begin{matrix} \overbrace{}^{li} & \overbrace{}^{li} & \overbrace{}^{j-2li} & \overbrace{}^{j\to\infty} \end{matrix} \begin{matrix} li\{ \\ li\{ \\ \\ \end{matrix} \begin{pmatrix} R_{11} & 0 & 0 \\ R_{21} & R_{22} & 0 \end{pmatrix} \begin{matrix} Q_1^T \}li \\ Q_2^T \}li \\ Q_3^T \}j-2li \end{matrix} = R_{21} Q_1^T \tag{14}$$

where $(.)^{\dagger}$ denotes the Moore-Penrose pseudo-inverse of a matrix.

(3) Singular value decomposition of the projection.

$$\mathrm{P}_i = USV^T = \begin{pmatrix} U_1 & U_2 \end{pmatrix} \begin{pmatrix} S_1 & 0 \\ 0 & S_2 = 0 \end{pmatrix} \begin{pmatrix} V_1 \\ V_2 \end{pmatrix} = U_1 S_1 V_1^T \tag{15}$$

(4) Deduce the extended observability matrix O_i and Kalman filter state sequence $\hat{X}_i$.

$$\mathrm{P}_i = Y_f / Y_p = \begin{pmatrix} R_i & R_{i-1} & \ldots & R_1 \\ R_{i+1} & R_i & \ldots & R_2 \\ \ldots & \ldots & \ldots & \ldots \\ R_{2i-1} & R_{2i-2} & \ldots & R_i \end{pmatrix} \begin{pmatrix} R_0 & R_{-1} & \ldots & R_{1-i} \\ R_1 & R_0 & \ldots & R_{2-i} \\ \ldots & \ldots & \ldots & \ldots \\ R_{i-1} & R_{i-2} & \ldots & R_0 \end{pmatrix} Y_p = \begin{pmatrix} C \\ CA \\ \cdots \\ CA^{i-1} \end{pmatrix} \begin{pmatrix} \hat{x}_i & \hat{x}_{i+1} & \cdots & \hat{x}_{i+j-1} \end{pmatrix} = O_i \hat{X}_i \tag{16}$$

where

$$O_i = U_1 S_1^{1/2}, \quad \hat{X}_i = O_i^{\dagger} \mathrm{P}_i \tag{17}$$

(5) Estimate the system matrices A and C.

A new way of division is conducted on the Hankel matrix in Eq. (4).

$$\begin{pmatrix} Y_{0|i} \\ \hline Y_{i+1|2i-1} \end{pmatrix} = \begin{pmatrix} Y_p^+ \\ \hline Y_f^- \end{pmatrix} \tag{18}$$

Another projection $P_{i\text{-}1}$ is computed for the sake of $\hat{X}_{i+1}$.

$$\mathrm{P}_{i-1} = Y_f^- / Y_p^+ = O_{i-1}\hat{X}_{i+1} \tag{19}$$

$$\hat{X}_{i+1} = O_{i-1}^{\dagger}\mathrm{P}_{i-1} \tag{20}$$

Then, $\hat{X}_i$ and $\hat{X}_{i+1}$ are substituted into the stochastic state space model, and the system matrices A and C are estimated in a least square sense, where V_i and W_i are the residuals.

$$\begin{pmatrix} \hat{X}_{i+1} \\ Y_{i\mid i} \end{pmatrix} = \begin{pmatrix} A \\ C \end{pmatrix}\hat{X}_i + \begin{pmatrix} W_i \\ V_i \end{pmatrix} \Rightarrow \begin{pmatrix} A \\ C \end{pmatrix} = \begin{pmatrix} \hat{X}_{i+1} \\ Y_{i\mid i} \end{pmatrix}\hat{X}_i^{\dagger} \tag{21}$$

(6) Identify modal parameters from A and C, similarly as the covariance-driven method.

2.4 Stabilization diagram

It is difficult to determine the exact order of system for singular value decomposition and to get clear results of structural modal parameters in practical application because of the numerical and ambient noises. Therefore, the stabilization diagram has been introduced. The poles corresponding to a certain model order are compared to those of the one-order-lower model. As the model order increases, spurious frequencies from numerical and ambient noises would not stabilize according to the preset limits of modal parameters (Peeters 2000).

3. Improved stochastic subspace identification based on a delay index

Since practical ambient excitations of engineering structures under operational conditions are not always white noises, the traditional stochastic subspace identification should be improved in order to relax the stationary-white-noise assumption of inputs and eliminate the spurious modes caused by non-white noise excitations in identification results. Those non-white noise ambient excitation sources might be various and mixed, and it is unrealistic to consider all of their potential forms. This paper focuses on the stationary non-white noise ambient inputs whose autocorrelations are not zero near the vertical axis. It is a simple but representative kind of non-white noises, involving many forms of practical non-white noise ambient excitations in time domain, like colored noises, swept harmonics, impacts, and so on. The specific functions of stationary-white-noise assumption in the traditional stochastic subspace identification are investigated. Then, for the aforementioned non-white noise ambient excitations, a delay index is introduced to modify the covariance-driven and data-driven stochastic subspace identification methods respectively. Furthermore, the determination of delay index is discussed for practical applications.

3.1 The functions of stationary-white-noise assumption in traditional methods

On the basis of the stationary-white-noise assumption in Eq. (2), the recursive relationship between output covariances and system state matrix, namely $R_i=CA^{i-1}G$ in Eq. (3), is established. It plays a key role in the traditional stochastic subspace identification by relating the measured vibration measurements to the dynamic characteristics of structural system.

$$
\begin{aligned}
R_1 &= \mathrm{E}\left[y_{k+1} y_k^T \right] \\
&= \mathrm{E}\left[C x_{k+1} y_k^T + v_{k+1} x_k^T C^T + v_{k+1} v_k^T \right] \\
&= CG + \mathrm{E}\left[v_{k+1} x_k^T \right] C^T + \mathrm{E}\left[v_{k+1} v_k^T \right] \\
R_2 &= \mathrm{E}\left[y_{k+2} y_k^T \right] \\
&= \mathrm{E}\left[CA x_{k+1} y_k^T + C w_{k+1} x_k^T C^T + v_{k+2} x_k^T C^T + C w_{k+1} v_k^T + v_{k+2} v_k^T \right] \\
&= CAG + C\,\mathrm{E}\left[w_{k+1} x_k^T \right] C^T + \mathrm{E}\left[v_{k+2} x_k^T \right] C^T + C\,\mathrm{E}\left[w_{k+1} v_k^T \right] + \mathrm{E}\left[v_{k+2} v_k^T \right] \qquad (22) \\
&\cdots \\
R_i &= \mathrm{E}\left[y_{k+i} y_k^T \right] \\
&= \mathrm{E}\left[CA^{i-1} x_{k+1} y_k^T + \left(CA^{i-2} w_{k+1} + \cdots + CA w_{k+i-2} + C w_{k+i-1} + v_{k+i} \right) \left(C x_k + v_k \right)^T \right] \\
&= CA^{i-1} G + CA^{i-2}\,\mathrm{E}\left[w_{k+1} x_k^T \right] C^T + \cdots + CA\,\mathrm{E}\left[w_{k+i-2} x_k^T \right] C^T + C\,\mathrm{E}\left[w_{k+i-1} x_k^T \right] C^T \\
&\quad + \mathrm{E}\left[v_{k+i} x_k^T \right] C^T + CA^{i-2}\,\mathrm{E}\left[w_{k+1} v_k^T \right] + \cdots + CA\,\mathrm{E}\left[w_{k+i-2} v_k^T \right] C^T + C\,\mathrm{E}\left[w_{k+i-1} v_k^T \right] + \mathrm{E}\left[v_{k+i} v_k^T \right]
\end{aligned}
$$

Here, $\mathrm{E}[w_{k+1} x_k^T]$ to $\mathrm{E}[w_{k+i-1} x_k^T]$, $E[v_{k+i} x_k^T]$, $\mathrm{E}[w_{k+1} v_k^T]$ to $\mathrm{E}[w_{k+i-1} v_k^T]$, and $E[v_{k+i} v_k^T]$ are equal to zeros only under the stationary-white-noise assumption, which ensures w_k and v_k to be zero-mean white noise vector sequences, and independent of state vector x_k.

With this recursive relationship, it is then possible to achieve structural characteristics through singular value decomposition of the covariance matrix (covariance-driven method) or projection matrix (data-driven method) (Van Overschee and De Moor 1996, Peeters 2000). Thus, in order to relax the stationary-white-noise assumption of ambient excitations, a delay index could be introduced into the Hankel matrix to suppress the influence of unqualified output covariances of this recursive relationship.

3.2 Improved covariance-driven stochastic subspace identification

For stationary non-white noise ambient excitations with nonzero autocorrelations in time interval $[-t_0, t_0]$, the recursive relationship in Eq. (3) can only start from R_{x+1}, where $x=t_0 \times f_s$ (f_s is the sampling rate) is called the delay index. In order to avoid those unqualified covariances, R_1 to R_x, a delay index x is introduced into the Hankel matrix to get rid of the corresponding unqualified elements, i.e., deleting the first x rows at the front of traditional future part Y_f (as shown in Eq. (4)) and adding another x rows at its end. Thus, the Hankel matrix becomes

$$
\begin{pmatrix} \dfrac{Y_{0|i-1}}{Y_{x+i|x+2i-1}} \end{pmatrix} = \begin{pmatrix} \dfrac{Y_p}{Y_f} \end{pmatrix} = \frac{1}{\sqrt{j}} \left(\begin{array}{ccccc}
y_0 & y_1 & y_2 & \cdots & y_{j-1} \\
y_1 & y_2 & y_3 & \cdots & y_j \\
\cdots & \cdots & \cdots & \cdots & \cdots \\
y_{i-1} & y_i & y_{i+1} & \cdots & y_{i+j-2} \\
\hline
y_{x+i} & y_{x+i+1} & y_{x+i+2} & \cdots & y_{x+i+j-1} \\
y_{x+i+1} & y_{x+i+2} & y_{x+i+3} & \cdots & y_{x+i+j} \\
\cdots & \cdots & \cdots & \cdots & \cdots \\
y_{x+2i-1} & y_{x+2i} & y_{x+2i+1} & \cdots & y_{x+2i+j-2}
\end{array} \right) \qquad (23)
$$

The Toeplitz matrix includes R_{x+1}, R_{x+2},... R_{x+2i-1}, instead of R_1, R_2,...,R_{2i-1}.

$$T_{x+1|x+i} = Y_f Y_p^T = \begin{pmatrix} R_{x+i} & R_{x+i-1} & ... & R_{x+1} \\ R_{x+i+1} & R_{x+i} & ... & R_{x+2} \\ ... & ... & ... & ... \\ R_{x+2i-1} & R_{x+2i-2} & ... & R_{x+i} \end{pmatrix} = \begin{pmatrix} CA^x \\ CA^{x+1} \\ \cdots \\ CA^{x+i-1} \end{pmatrix} \begin{pmatrix} A^{i-1}G & ... & A^1G & G \end{pmatrix} = \bar{O}_i \Gamma_i \tag{24}$$

where the reversed extended stochastic controllability matrix Γ_i remains the same as that of traditional identification process, while the extended observability matrix $\bar{O}_i$ changes to be

$$\bar{O}_i = \begin{pmatrix} CA^x & CA^{x+1} & \cdots & CA^{x+i-1} \end{pmatrix}^T \tag{25}$$

For an observable and controllable structural system, the rank n is computed by singular value decomposition of the block Toeplitz matrix $T_{x+1|x+i}$.

$$T_{x+1|x+i} = USV^T = \begin{pmatrix} U_3 & U_4 \end{pmatrix} \begin{pmatrix} S_3 & 0 \\ 0 & S_4 = 0 \end{pmatrix} \begin{pmatrix} V_3 \\ V_4 \end{pmatrix} = U_3 S_3 V_3^T \tag{26}$$

By comparing Eq. (24) with Eq. (26), the matrices $\bar{O}_i$ and Γ_i respectively yield

$$\bar{O}_i = U_3 S_3^{1/2}, \quad \Gamma_i = S_3^{1/2} V_3^T \tag{27}$$

In the same way, another Toeplitz matrix is calculated from Hankel matrix ($Y_{0|i-1}/Y_{x+i+1|x+2i}$), and decomposed as

$$T_{x+2|x+i+1} = \bar{O}_i A \Gamma_i \tag{28}$$

Utilizing these two Toeplitz matrices, the state matrix of a vibrating system is achieved by

$$A = S_3^{1/2} U_3^T T_{x+2|x+i+1} V_3 S_3^{1/2} \tag{29}$$

Then, the rest of identification procedures remain the same as the traditional covariance-driven stochastic subspace identification as stated in section 2.2.

3.3 Improved data-driven stochastic subspace identification

Similarly, the concept of delay index is introduced to the data-driven stochastic subspace identification. Although the computation of output covariances is replaced by projecting the row space of future outputs into that of past outputs here, the influence of non-white noise ambient excitations can still be removed by avoiding the corresponding unqualified elements in Hankel matrix. The Hankel matrix ($Y_{0|i-1}/Y_{x+i|x+2i-1}$) with a delay index x in Eq. (23) is formulated first, whose QR decomposition yields the projection P_i.

$$\mathrm{P}_i = Y_f / Y_p = \begin{pmatrix} R_{x+i} & R_{x+i-1} & ... & R_{x+1} \\ R_{x+i+1} & R_{x+i} & ... & R_{x+2} \\ ... & ... & ... & ... \\ R_{x+2i-1} & R_{x+2i-2} & ... & R_{x+i} \end{pmatrix} \begin{pmatrix} R_0 & R_{-1} & ... & R_{1-i} \\ R_1 & R_0 & ... & R_{2-i} \\ ... & ... & ... & ... \\ R_{i-1} & R_{i-2} & ... & R_0 \end{pmatrix} Y_p = \begin{pmatrix} CA^x \\ CA^{x+1} \\ \cdots \\ CA^{x+i-1} \end{pmatrix} \begin{pmatrix} \hat{x}_i & \hat{x}_{i+1} & \cdots & \hat{x}_{i+j-1} \end{pmatrix} = \bar{O}_i \hat{X}_i \tag{30}$$

where the extended observability matrix $\overline{O}_i$ has been specified in Eq. (25).

The singular value decomposition of P_i is then calculated

$$\mathrm{P}_i = USV^T = \begin{pmatrix} U_3 & U_4 \end{pmatrix} \begin{pmatrix} S_3 & 0 \\ 0 & S_4 = 0 \end{pmatrix} \begin{pmatrix} V_3 \\ V_4 \end{pmatrix} = U_3 S_3 V_3^T \tag{31}$$

By comparing Eq. (30) with Eq. (31), the matrices $\overline{O}_i$ and $\hat{X}_i$ respectively yield

$$\overline{O}_i = U_3 S_3^{1/2}, \quad \hat{X}_i = O_i^{\dagger} \mathrm{P}_i \tag{32}$$

For the sake of system identification, another Hankel matrix ($Y_{0|i}/Y_{x+i+1|x+2i-1}$) composed of Y_p^+ and Y_f^- is formulated, and one more projection P_{i-1} is done to get $\hat{X}_{i+1}$.

$$\begin{pmatrix} \dfrac{Y_{0|i}}{Y_{x+i+1|x+2i-1}} \end{pmatrix} = \begin{pmatrix} \dfrac{Y_p^+}{Y_f^-} \end{pmatrix} = \frac{1}{\sqrt{j}} \left(\begin{array}{ccccc} y_0 & y_1 & y_2 & \cdots & y_{j-1} \\ y_1 & y_2 & y_3 & \cdots & y_j \\ \cdots & \cdots & \cdots & \cdots & \cdots \\ y_{i-1} & y_i & y_{i+1} & \cdots & y_{i+j-2} \\ y_i & y_{i+1} & y_{i+2} & \cdots & y_{i+j-1} \\ \hline y_{x+i+1} & y_{x+i+2} & y_{x+i+3} & \cdots & y_{x+i+j} \\ \cdots & \cdots & \cdots & \cdots & \cdots \\ y_{x+2i-1} & y_{x+2i} & y_{x+2i+1} & \cdots & y_{x+2i+j-2} \end{array} \right) \tag{33}$$

$$\mathrm{P}_{i-1} = Y_f^- / Y_p^+ = \overline{O}_{i-1} \hat{X}_{i+1} \tag{34}$$

$$\hat{X}_{i+1} = \overline{O}_{i-1}^{\dagger} \mathrm{P}_{i-1} \tag{35}$$

Then, the rest of identification procedures remain the same as the traditional data-driven stochastic subspace identification stated in section 2.3.

3.4 Determination of the delay index

The improved stochastic subspace identification based on a delay index excludes those nonzero autocorrelations. Thus, the spurious modes are eliminated and the precision of identification results is improved accordingly. The delay index x is just the number of samples in half of the time interval with nonzero values of autocorrelation function. It should be noted that the traditional stochastic subspace identification is in fact the case of delay index x=0. However, actual ambient excitations are unmeasured that could be very complicated. It is difficult to determine the exact values of delay index x for various operational vibration measurements in practice. Similar to the idea of stabilization diagram, several different values could be attempted for the delay index x with an ascending order, and the modal parameters of structural system are calculated sequentially using the improved stochastic subspace identification. All the identified stabilization diagrams corresponding to different values of delay index are then compared to determine whether the delay index is necessary and what is its appropriate value if needed. If a pole could not keep stable in different stabilization diagrams as the value of delay index increases, it should be a spurious mode irrelevant to the structural system. Also, the delay index could not be too large because it is considered that lower lag correlations (R_i with smaller i value) contain more accurate information

of structural system than higher lag correlation (R_i with larger i value). Based on the experiences of this research, it normally would not exceed 10% of the length of measurement data analyzed.

4. Numerical verification

A 2D four-story frame with lumped masses, as shown in Fig. 1, was simulated to demonstrate the performance of proposed method in operational modal analysis under non-white noise ambient excitations. Rayleigh dampings were assumed for its four modes. Simulated acceleration excitations were inputted through the foundation, and acceleration responses at all stories (a_1, a_2, a_3, and a_4) were calculated by the Newmark-Beta method. The sampling rate was 200 Hz, and the sampling time was 100 s. Then, the calculated acceleration responses were taken as operational measurements to identify the modal parameters using both of the traditional and improved covariance-driven stochastic subspace identification methods.

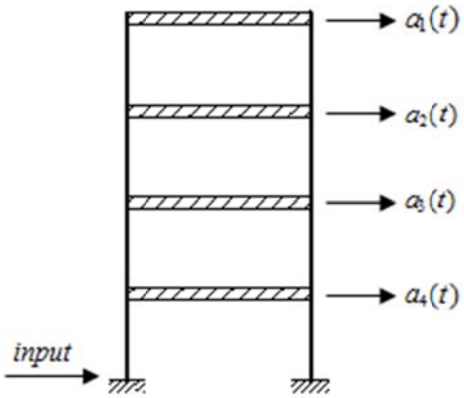

Fig. 1 Four-story frame

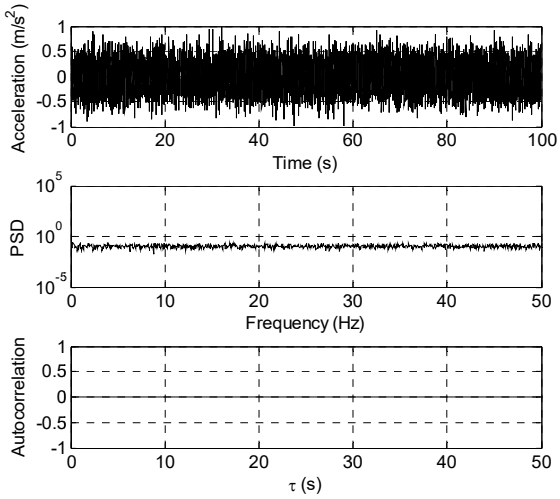

Fig. 2 White noise input of simulation C1

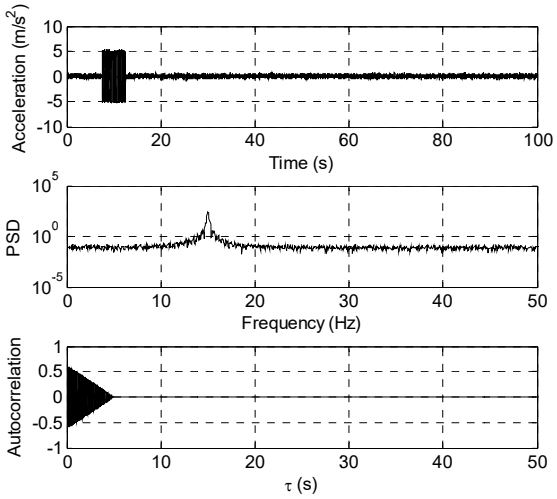

Fig. 3 Non-white noise input of simulation C2

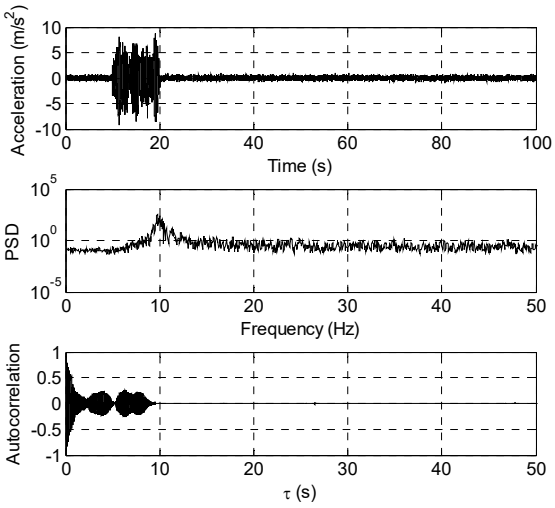

Fig. 4 Non-white noise input of simulation C3

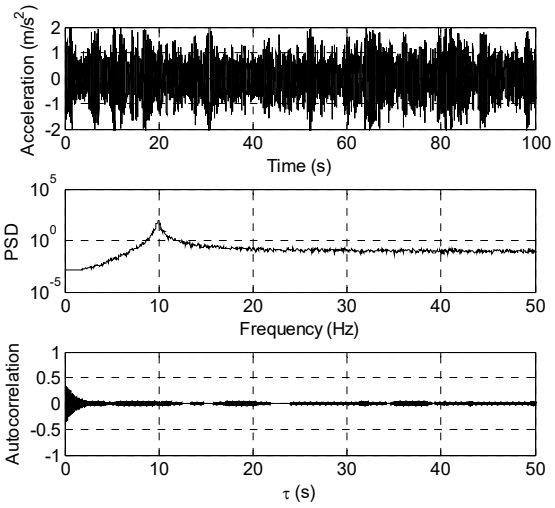

Fig. 5 Non-white noise input of simulation C4

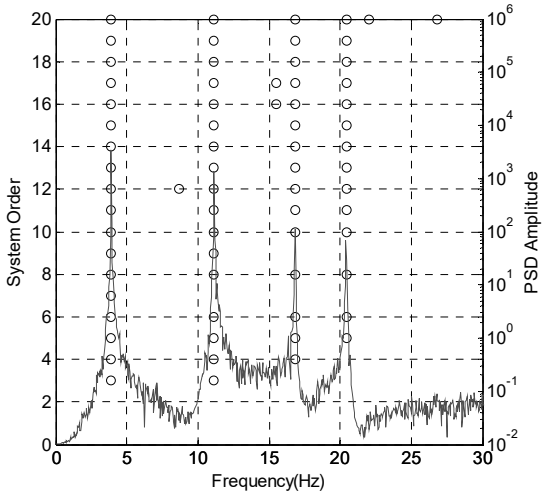

Fig. 6 Stabilization diagram of simulation C1

Four cases were simulated with different forms of excitations respectively.

• C1: white noise excitation as a benchmark for comparison, which is shown in Fig. 2 with its PSD and autocorrelation functions (τ is the time lag in second).

• C2: non-white noise excitation by adding a 5 s harmonic wave of 15 Hz into a white noise process, which is shown in Fig. 3 with its PSD and autocorrelation functions.

• C3: non-white noise excitation by adding a 10 s colored noise of 10 Hz into a white noise process. The colored noise itself was generated from a white noise filtered by a single-degree-of-freedom system with natural frequency of 10 Hz and damping ratio of 5%. The excitation is shown in Fig. 4 with its PSD and autocorrelation functions.

• C4: non-white noise excitation by combing a colored noise of 10 Hz with a white noise process. The colored noise was also generated from a white noise filtered by a single-degree-of-

freedom system with natural frequency of 10 Hz and damping ratio of 5%. The excitation is shown in Fig. 5 with its PSD and autocorrelation functions.

In the benchmark case C1, four natural frequencies of this frame have been obtained using the traditional stochastic subspace identification (i.e., improved stochastic subspace identification with delay index x=0): f_1=3.90 Hz, f_2=11.14 Hz, f_3=16.84 Hz, and f_4=20.42 Hz. The corresponding stabilization diagram is displayed in Fig. 6, together with the PSD of a selected acceleration response a_3.

In C2 with non-white noise input, considered as the unknown ambient excitation, the delay

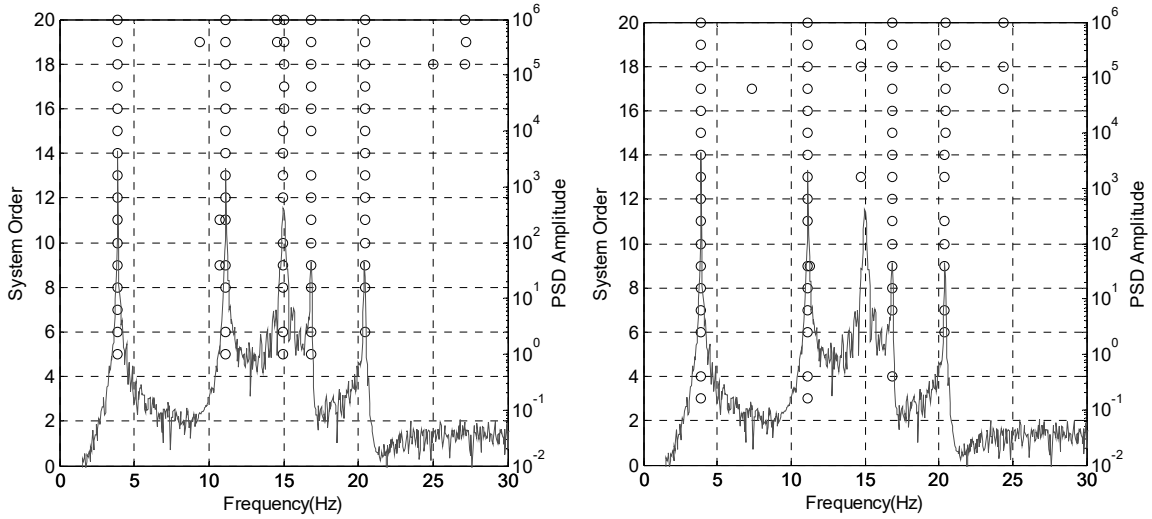

(a) Traditional SSI (b) Improved SSI

Fig. 7 Stabilization diagrams of simulation C2

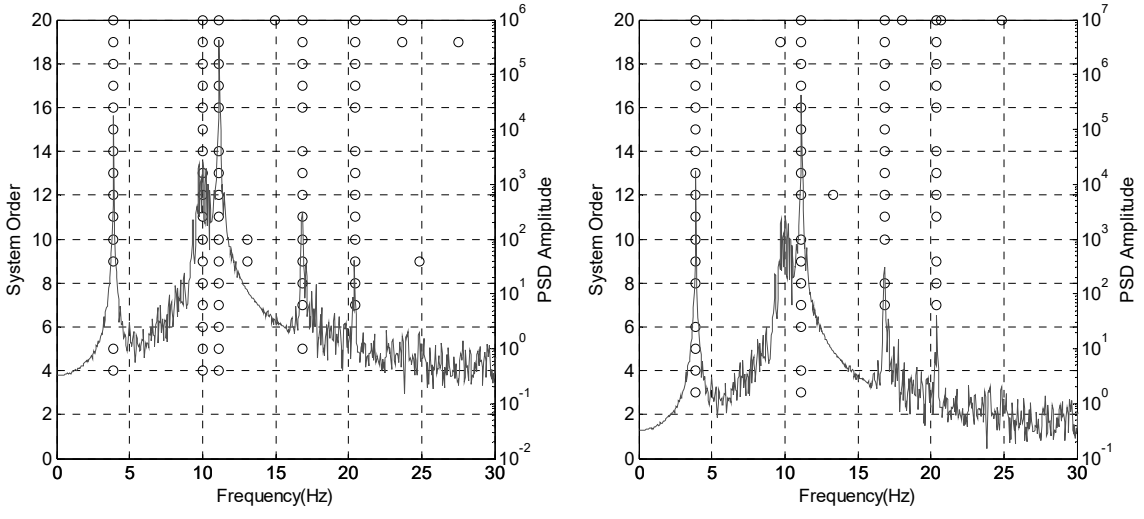

(a) Traditional SSI (b) Improved SSI

Fig. 8 Stabilization diagrams of simulation C3

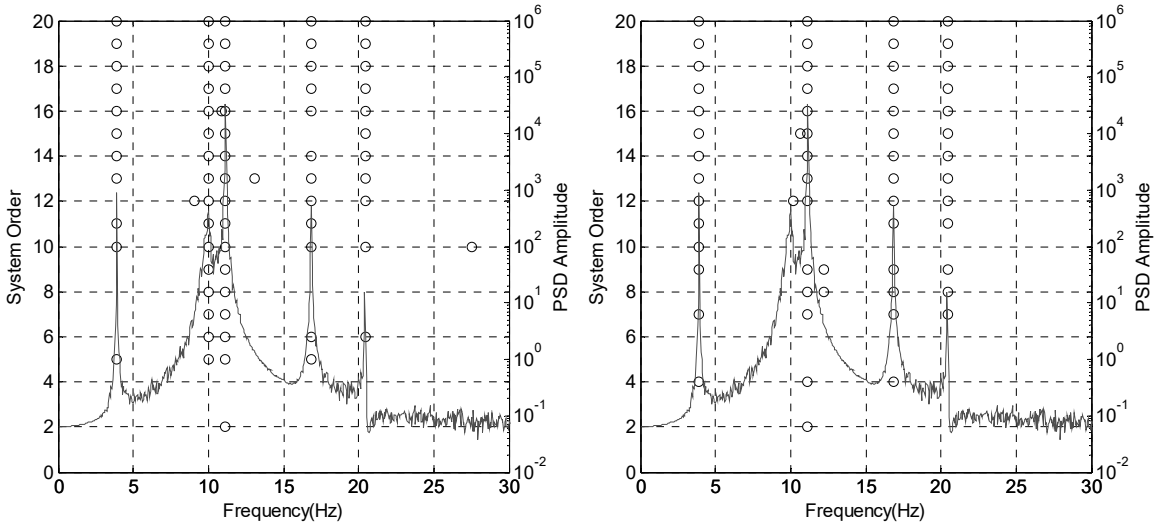

(a) Traditional SSI (b) Improved SSI

Fig. 9 Stabilization diagrams of simulation C4

index for improved stochastic subspace identification was determined to be 1000 after attempting several times of x=500, 1000, and 1500, according to principles stated in section 3.4. The stabilization diagrams obtained by traditional and improved identification methods are compared in Fig. 7. As can be seen, the spurious mode arises in the traditional stabilization diagram due to non-white component 15 Hz in the excitation, whereas it is successfully rejected after introducing the delay index.

In C3 with non-white noise input, the delay index for improved stochastic subspace identification was determined to be 2000. The stabilization diagrams obtained by traditional and improved identification methods are compared in Fig. 8. The improved stochastic subspace identification based on a delay index can accurately distinguish structural modes from the spurious mode due to a non-white component of 10 Hz in excitation, even if it is close to the second structural mode.

In C4, the autocorrelation function of excitation has relative higher absolute values in both neighborhood of vertical axis and range of time lag τ>60 s, and its small values in the middle range can be approximately considered to be zeros. Because the autocorrelations of too long time lags, i.e., τ>60 s, would not be involved in the calculation of stochastic subspace identification, the improved method proposed still applies to this type of excitations. The delay index was determined to be 1000 after attempts and comparison of x=500, 1000, and 1500, and the corresponding stabilization diagram is shown in Fig. 9 (b), following that of the traditional method in Fig. 9 (a). It is obvious that the delay index helps to eliminate the spurious mode of 10 Hz.

Finally, frequencies identified in the four cases by both traditional and improved stochastic subspace identification methods are summarized in Table 1. The improved stochastic subspace identification reveals its advantages over eliminating spurious modes caused by non-white noise excitations, even if some of them are close to the structural modes. And the structural modes identified in the cases of non-white noise inputs are accurate as that in the case of white noise input.

Table 1 Identified frequencies of different cases in the simulation (unit: Hz)

Structural Mode Number	C1	C2		C3		C4	
		Traditional SSI	Improved SSI	Traditional SSI	Improved SSI	Traditional SSI	Improved SSI
1	3.90	3.90	3.90	3.90	3.90	3.90	3.90
--	--	--	--	10.00	--	10.00	--
2	11.14	11.14	11.14	11.14	11.14	11.14	11.14
--	--	15.00	--				
3	16.84	16.85	16.84	16.82	16.85	16.84	16.84
4	20.42	20.42	20.42	20.43	20.41	20.43	20.42

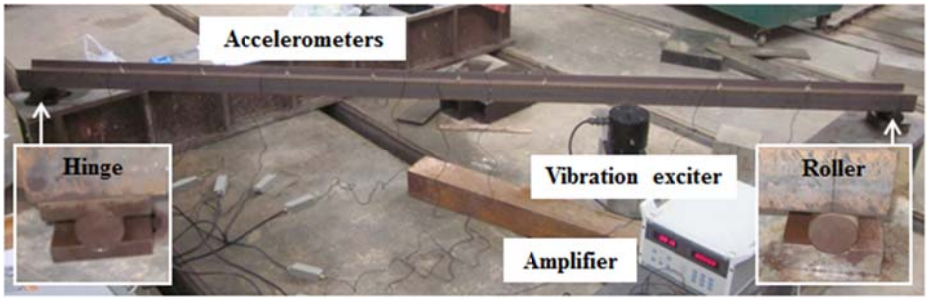

Fig. 10 Simply supported steel beam tested in the laboratory

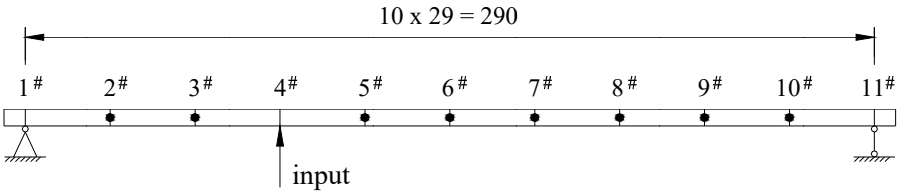

Fig. 11 Location of sensors and excitation (unit: cm)

5. Experimental verification

Various non-white noise excitations were imposed on a simply supported steel beam in the laboratory, as shown in Fig. 10, to further examine the feasibility of improved stochastic subspace identification. The beam had a span of 2.9m with a uniform H section. The elastic modulus was E=206 GPa, and the density was ρ=7850 kg/m^3. Different non-white noise excitations were numerically generated, and physically applied through a function/arbitrary waveform generator (33521A by Agilent Technologies), a power amplifier, and a vibration exciter (JZQ-50). The maximum exciting force of vibration exciter was 50 N, maximum amplitude was ±5 mm, and frequency range covered 10 - 3000 Hz. The span of tested beam was divided equally by 11 nodes, as shown in Fig. 11. The excitations were imposed at node 4#. And eight accelerometers were installed on the beam to collect vertical accelerations at the nodes except for both supports and excitation node. Vibration output signals were recorded by the DH5923 dynamic data acquisition

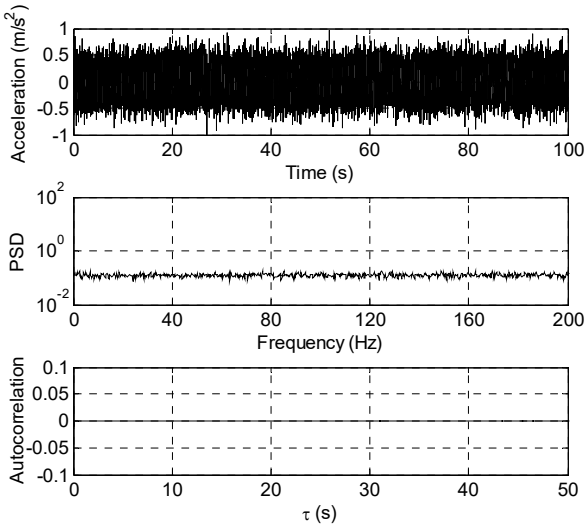

Fig. 12 White noise excitation of experiment C1

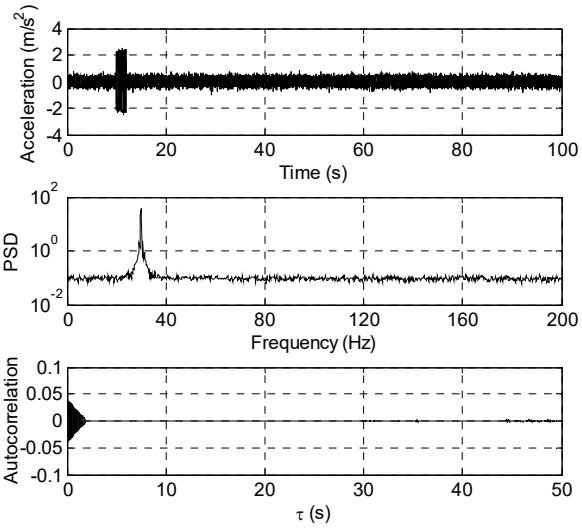

Fig. 13 Non-white noise excitation of experiment C2

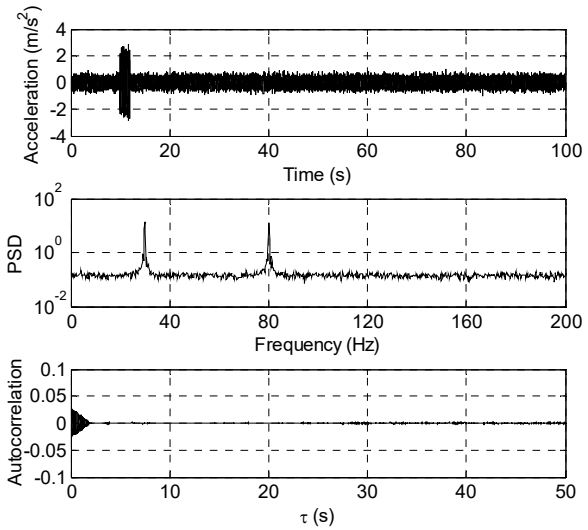

Fig. 14 Non-white noise excitation of experiment C3

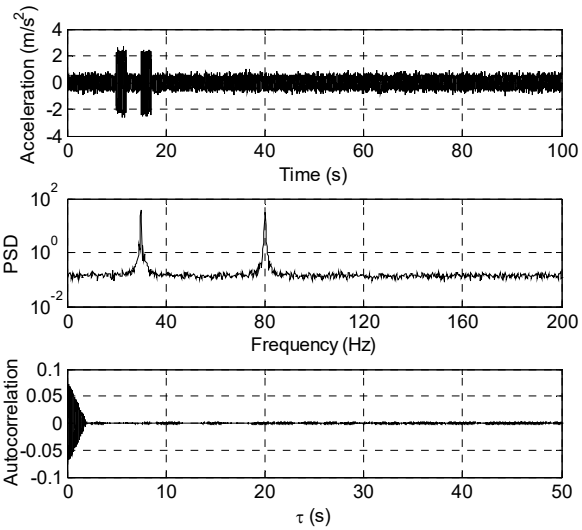

Fig. 15 Non-white noise excitation of experiment C4

system, supplied by Donghua Testing Technology Co., LTD. The sampling rate was 1000 Hz, and the sampling time was 100 s. Moreover, the excitation force from vibration exciter should be carefully controlled to be moderate during experiments. Too small force could not excite all structural modes interested, while too large force would work as a redundant support to the beam, and might make the testing system overloaded.

Four cases of excitations were set up respectively as below.

• C1: benchmark test with white noise excitation, which is shown in Fig. 12 with its power spectral density (PSD) and autocorrelation functions.

• C2: non-white noise excitation by adding a 2 s harmonic wave of 30 Hz into a white noise

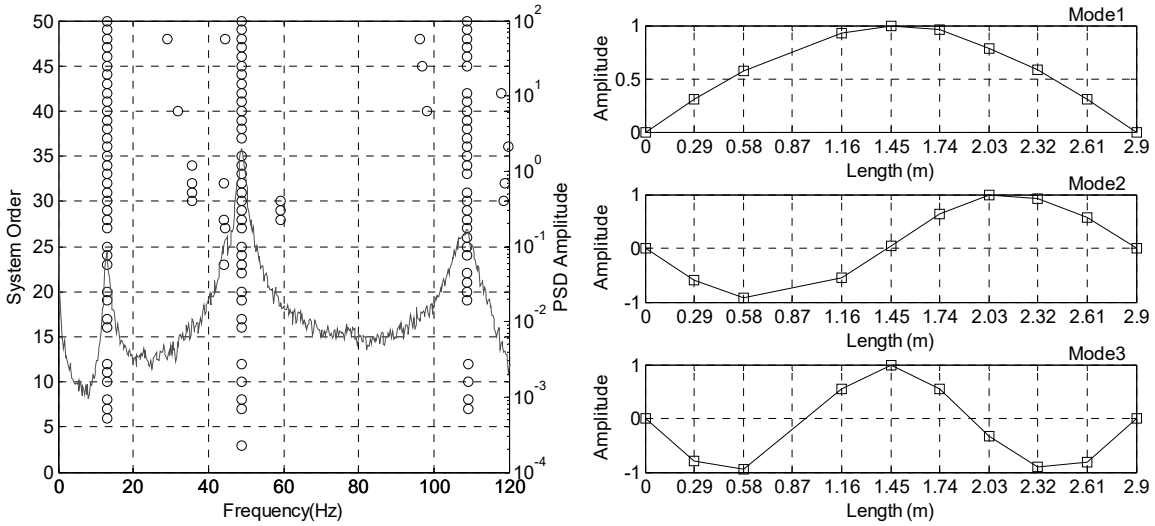

(a) Frequencies (b) Mode shapes

Fig. 16 Identified modal parameters of tested beam in experiment C1

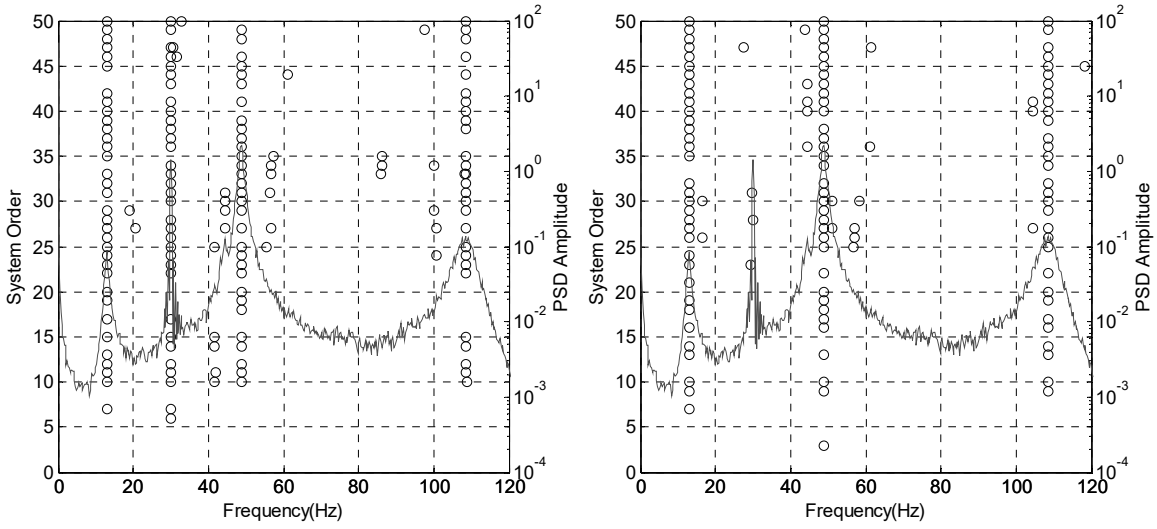

(a) Traditional SSI (b) Improved SSI

Fig. 17 Stabilization diagrams of experiment C2

process, which is shown in Fig. 13 with its PSD and autocorrelation functions.

• C3: non-white noise excitation by adding a 2 s harmonic wave of 30 Hz and a 2 s harmonic wave of 80 Hz simultaneously into a white noise process, which is shown in Fig. 14 with its PSD and autocorrelation functions.

• C4: non-white noise excitation by adding a 2 s harmonic wave of 30 Hz and a 2 s harmonic wave of 80 Hz separately into a white noise process, which is shown in Fig. 15 with its PSD and autocorrelation functions.

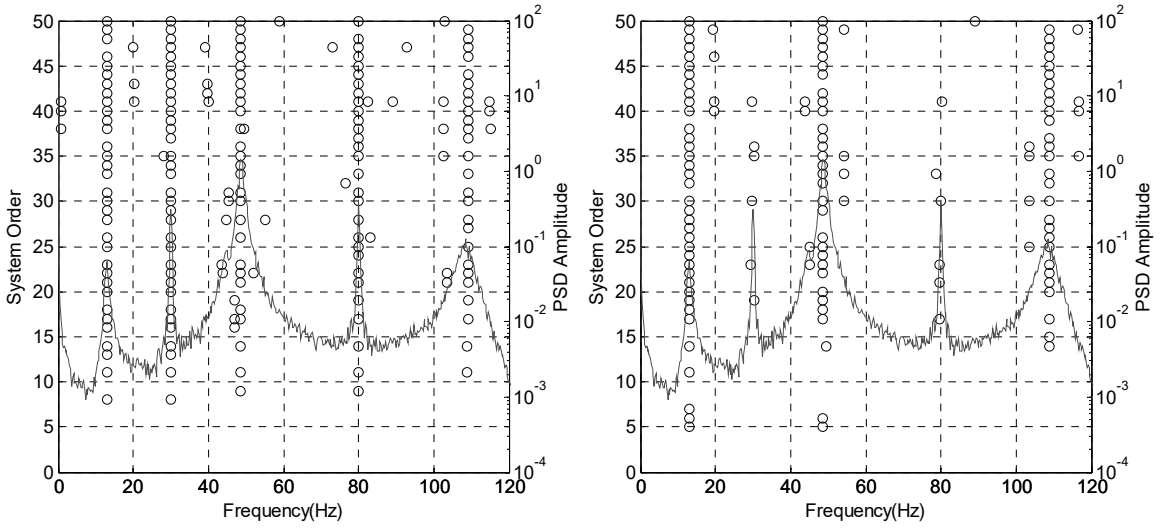

(a) Traditional SSI (b) Improved SSI

Fig. 18 Stabilization diagrams of experiment C3

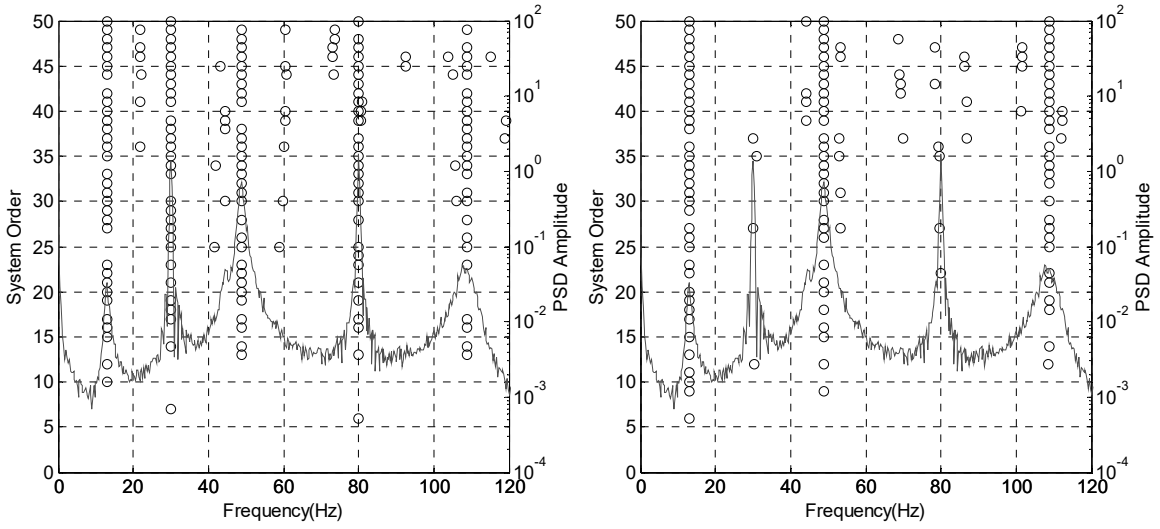

(a) Traditional SSI (b) Improved SSI

Fig. 19 Stabilization diagrams of experiment C4

It should be noted that these excitations were actually continuously repeated when applied on the beam. This makes the excitations to be stationary and more realistic, since the non-white noise components of excitations do repeated in practice.

The acceleration measurements were analyzed using both of the traditional and improved data-driven stochastic subspace identification methods. From the benchmark case C1, the first three natural frequencies of the beam tested were identified to be f_1=12.94 Hz, f_2=48.83 Hz, and f_3=108.90 Hz, with their corresponding mode shapes displayed in Fig. 16. In the other three cases

Table 2 Identified frequencies of different cases in the laboratory test (unit: Hz)

Structural Mode Number	C1	C2		C3		C4	
		Traditional SSI	Improved SSI	Traditional SSI	Improved SSI	Traditional SSI	Improved SSI
1	12.94	12.95	12.94	12.96	12.95	12.94	12.94
--	--	30.00	--	30.00	--	30.00	--
2	48.83	48.81	48.83	48.65	48.60	48.80	48.82
--	--	--	--	80.00	--	80.00	--
3	108.90	108.68	108.62	109.10	108.96	108.79	108.91

with non-white noise excitations, C2-C4, delay indexes were all determined to be 2000 after attempting several times of x=1000, 2000, and 3000. The stabilization diagrams of both traditional and improved stochastic subspace identification methods are respectively shown in Figs. 17-19. Table 2 summarizes all the frequency identification results of four cases. As can be seen, the non-white components 30 Hz and 80 Hz of excitations give rise to spurious modes in stabilization diagrams of the traditional stochastic subspace identification. However, the proposed improved stochastic subspace identification based on a delay index can effectively avoid these spurious modes, and works well no matter whether one or multiple non-white components exist simultaneously in the excitations. Under disturbance of non-white components, the identification errors of structural modes are within 2% using the improved stochastic subspace identification.

6. Conclusions

Due to heavy traffic, wind gusts, and other disturbances, actual ambient excitation sources of engineering structures under operational condition are often mixed with some obvious dominant frequencies, which violate the stationary-white-noise assumption of inputs in traditional operational modal analysis. For a representative kind of practical stationary non-white noise ambient excitations whose autocorrelations are not zero near the vertical axis, the improved stochastic subspace identification based on a delay index is proposed in this paper. By avoiding corresponding unqualified elements in the Hankel matrix, it relaxes the stationary-white-noise assumption of inputs, and eliminates the spurious modes due to non-white components in ambient excitations. Numerical simulations on a four-story frame and vibration experiments on a simply supported beam have confirmed the accuracy and reliability of proposed improved stochastic subspace identification.

The non-white noise excitations applied in both numerical and experimental verifications are simple forms, by adding harmonic waves and colored noises into white noise processes. In fact, cases under non-white noise ambient excitations with nonzero autocorrelation values near the vertical axis, however they behave in time and frequency domains and whether non-white frequency components contained are close to the structural modes, would all benefit from this improved stochastic subspace identification based on a delay index for successful rejection of spurious modes. For practical application, several values of the delay index need to be attempted in order to determine the most appropriate one, and meanwhile their corresponding stabilization diagrams are compared to eliminate unstable spurious modes. Besides, including more types of

non-white noise ambient inputs of engineering structures under operational conditions is still one of the future research interests.

Acknowledgments

Financial support from the Natural Science Foundation of China under Grant Nos. 51278163 and 51308175 are acknowledged.

References

Araújo, I.G. and Laier, J.E. (2014), "Operational modal analysis using SVD of power spectral density transmissibility matrices", *Mech. Syst. Signal Pr.*, **46**(1), 129-145.

Brincker, R., Zhang, L.M. and Andersen, P. (2001), "Modal identification of output-only systems using frequency domain decomposition", *Smart Mater. Struct.*, **10**(3), 441-445.

Cooper, J.E., Desforges, M.J. and Wright, J.R. (1995), "Model parameter identification using an unknown coloured random input", *Mech. Syst. Signal Pr.*, **9**(6), 685-695.

De Roeck, G., Peeters, B. and Ren, W.X. (2000), "Benchmark study on system identification through ambient vibration measurements", *Proceedings of the 18th International Modal Analysis Conference (IMAC XVIII)*, San Antonio, TX, USA.

Devriendt, C., De Sitter, G., Vanlanduit, S. and Guillaume, P. (2009), "Operational modal analysis in the presence of harmonic excitations by the use of transmissibility measurements", *Mech. Syst. Signal Pr.*, **23**(3), 621-635.

Devriendt, C. and Guillaume, P. (2007), "The use of transmissibility measurements in output-only modal analysis", *Mech. Syst. Signal Pr.*, **21**(7), 2689-2696.

Dorvash, S. and Pakzad, S.N. (2012), "Effects of measurement noise on modal parameter identification", *Smart Mater. Struct.*, **21**(6), 065008.

Goethals, I., Vanluyten, B. and De Moor, B. (2004), "Reliable spurious mode rejection using self learning algorithms", *Proceedings of the International Conference on Noise and Vibration Engineering (ISMA 2004)*, Leuven, Belgium.

Goursat, M. and Mevel, L. (2008), "Covariance subspace identification: numerical analysis of spurious mode stability", *Proceedings of the 26th International Modal Analysis Conference (IMAC-XXVI)*, Orlando, US.

Hassiotis, S. (1999), "Identification of damage using natural frequencies and system moments", *Struct. Eng. Mech.*, **8**(3), 285-297.

Jacobsen, N.J. (2005), "Identifying harmonic components in operational modal analysis", *Proceedings of the 12th International Congress on Sound and Vibration (ICSV 12)*, Lisbon, Portugal.

Li, D., Ren, W.X. and Hu, Y.D. (2011), "Output-only modal parameter identification based on augmented state space models", *Proceedings of the 4th International Symposium on Innovation & Sustainability of Structures in Civil Engineering (ISISS 2011)*, Xiamen, China.

Lisowski, W. (2001), "Classification of vibration modes in operational modal analysis", *Proceedings of the International Conference on Structural System Identification*, Kassel, Germany.

Mevel, L., Benveniste, A., Basseville, M. and Goursat, M. (2002), "Blind subspace-based eigenstructure identification under nonstationary excitation using moving sensors", *IEEE T. Signal Pr.*, **50**(1), 41-48.

Mohanty, P. and Rixen, D.J. (2004a), "A modified Ibrahim time domain algorithm for operational modal analysis including harmonic excitation", *J. Sound Vib.*, **275**(1), 375-390.

Mohanty, P. and Rixen, D.J. (2004b), "Operational modal analysis in the presence of harmonic excitation", *J. Sound Vib.*, **270**(1-2), 93-109.

Mohanty, P. and Rixen, D.J. (2006), "Modified ERA method for operational modal analysis in the presence of harmonic excitations", *Mech. Syst. Signal Pr.*, **20**(1), 114-130.
Peeters, B. (2000), "System identification and damage detection in civil engineering", Ph.D. Dissertation, Katholieke Universiteit Leuven, Belgium.
Peeters, B. and De Roeck, G. (2001), "Stochastic system identification for operational modal analysis: a review", *J. Dyn. Syst., Meas., Control*, ASME, **123**(4), 659-667.
Ren, W.X., Zhao, T. and Harik, I.E. (2004), "Experimental and analytical modal analysis of steel arch bridge", *J. Struct. Eng*., ASCE, **130**(7), 1022-1031.
Ren, W.X. and Zong, Z.H. (2004), "Output-only modal parameter identification of civil engineering structures", *Struct. Eng. Mech*., **17**, 429-444.
Reynders, E. (2012), "System identification methods for (operational) modal analysis: review and comparison", *Arch. Comput. Meth. E*., **19**(1), 51-124.
Reynders, E., Pintelon, R. and De Roeck, G. (2008), "Uncertainty bounds on modal parameters obtained from stochastic subspace identification", *Mech. Syst. Signal Pr*., **22**(4), 948-969.
Saeed, K., Mechbal, N., Coffignal, G. and Verge, M. (2008), "Recursive modal parameter estimation using output-only subspace identification for structural health monitoring", *Proceedings of the 16th Mediterranean Conference on Control and Automation*, IEEE, Ajaccio Corsica, France.
Van der Auweraer, H. and Hermans, L. (1999), "Structural model identification from real operating conditions", *J. Sound Vib*., **33**(1), 34-41.
Van Overschee, P. and De Moor, B. (1996), *Subspace Identification for Linear Systems: Theory, Implementation, Applications*, Kluwer Academic Publishers, Netherlands.
Yan, W.J. and Ren, W.X. (2013), "Use of continuous-wavelet transmissibility for structural operational modal analysis", *J. Struct. Eng*., ASCE, **139**(9), 1444-1456.
Yi, J.H. and Yun, C.B. (2004), "Comparative study on modal identification methods using output-only information", *Struct. Eng. Mech*., **17**(3), 445-466.
Yu, D.J. and Ren, W.X. (2005), "EMD-based stochastic subspace identification of structures from operational vibration measurements", *Eng. Struct*., **27**(12), 1741-1751.

CC